

## On temporal variations of the multi-TeV cosmic ray anisotropy using the Tibet III Air Shower Array

M. Amenomori<sup>1</sup>, X. J. Bi<sup>2</sup>, D. Chen<sup>3</sup>, S. W. Cui<sup>4</sup>, Danzengluobu<sup>5</sup>, L. K. Ding<sup>2</sup>,  
X. H. Ding<sup>5</sup>, C. Fan<sup>6,2</sup>, C. F. Feng<sup>6</sup>, Zhaoyang Feng<sup>2</sup>, Z. Y. Feng<sup>7</sup>, X. Y. Gao<sup>8</sup>,  
Q. X. Geng<sup>8</sup>, Q. B. Gou<sup>2</sup>, H. W. Guo<sup>5</sup>, H. H. He<sup>2</sup>, M. He<sup>6</sup>, K. Hibino<sup>9</sup>, N. Hotta<sup>10</sup>,  
Haibing Hu<sup>5</sup>, H. B. Hu<sup>2</sup>, J. Huang<sup>2</sup>, Q. Huang<sup>7</sup>, H. Y. Jia<sup>7</sup>, L. Jiang<sup>8,2</sup>, F. Kajino<sup>11</sup>,  
K. Kasahara<sup>12</sup>, Y. Katayose<sup>13</sup>, C. Kato<sup>14</sup>, K. Kawata<sup>3</sup>, Labaciren<sup>5</sup>, G. M. Le<sup>15</sup>, A. F. Li<sup>6</sup>,  
H. C. Li<sup>4,2</sup>, J. Y. Li<sup>6</sup>, C. Liu<sup>2</sup>, Y.-Q. Lou<sup>16</sup>, H. Lu<sup>2</sup>, X. R. Meng<sup>5</sup>, K. Mizutani<sup>12,17</sup>, J. Mu<sup>8</sup>,  
K. Munakata<sup>14</sup>, A. Nagai<sup>18</sup>, H. Nanjo<sup>1</sup>, M. Nishizawa<sup>19</sup>, M. Ohnishi<sup>3</sup>, I. Ohta<sup>20</sup>,  
S. Ozawa<sup>12</sup>, T. Saito<sup>21</sup>, T. Y. Saito<sup>22</sup>, M. Sakata<sup>11</sup>, T. K. Sako<sup>3</sup>, M. Shibata<sup>13</sup>, A. Shiomi<sup>23</sup>,  
T. Shirai<sup>9</sup>, H. Sugimoto<sup>24</sup>, M. Takita<sup>3</sup>, Y. H. Tan<sup>2</sup>, N. Tateyama<sup>9</sup>, S. Torii<sup>12</sup>, H. Tsuchiya<sup>25</sup>,  
S. Udo<sup>9</sup>, B. Wang<sup>2</sup>, H. Wang<sup>2</sup>, Y. Wang<sup>2</sup>, Y. G. Wang<sup>6</sup>, H. R. Wu<sup>2</sup>, L. Xue<sup>6</sup>,  
Y. Yamamoto<sup>11</sup>, C. T. Yan<sup>26</sup>, X. C. Yang<sup>8</sup>, S. Yasue<sup>27</sup>, Z. H. Ye<sup>28</sup>, G. C. Yu<sup>7</sup>, A. F. Yuan<sup>5</sup>,  
T. Yuda<sup>9</sup>, H. M. Zhang<sup>2</sup>, J. L. Zhang<sup>2</sup>, N. J. Zhang<sup>6</sup>, X. Y. Zhang<sup>6</sup>, Y. Zhang<sup>2</sup>, Yi Zhang<sup>2</sup>,  
Ying Zhang<sup>7,2</sup>, Zhaxisangzhu<sup>5</sup> and X. X. Zhou<sup>7</sup>

(The Tibet AS $\gamma$  Collaboration)

- 
- <sup>1</sup>Department of Physics, Hirosaki University, Hirosaki 036-8561, Japan.
- <sup>2</sup>Key Laboratory of Particle Astrophysics, Institute of High Energy Physics, Chinese Academy of Sciences, Beijing 100049, China.
- <sup>3</sup>Institute for Cosmic Ray Research, University of Tokyo, Kashiwa 277-8582, Japan.
- <sup>4</sup>Department of Physics, Hebei Normal University, Shijiazhuang 050016, China.
- <sup>5</sup>Department of Mathematics and Physics, Tibet University, Lhasa 850000, China.
- <sup>6</sup>Department of Physics, Shandong University, Jinan 250100, China.
- <sup>7</sup>Institute of Modern Physics, SouthWest Jiaotong University, Chengdu 610031, China.
- <sup>8</sup>Department of Physics, Yunnan University, Kunming 650091, China.
- <sup>9</sup>Faculty of Engineering, Kanagawa University, Yokohama 221-8686, Japan.
- <sup>10</sup>Faculty of Education, Utsunomiya University, Utsunomiya 321-8505, Japan.
- <sup>11</sup>Department of Physics, Konan University, Kobe 658-8501, Japan.
- <sup>12</sup>Research Institute for Science and Engineering, Waseda University, Tokyo 169-8555, Japan.
- <sup>13</sup>Faculty of Engineering, Yokohama National University, Yokohama 240-8501, Japan.
- <sup>14</sup>Department of Physics, Shinshu University, Matsumoto 390-8621, Japan.
- <sup>15</sup>National Center for Space Weather, China Meteorological Administration, Beijing 100081, China.
- <sup>16</sup>Physics Department and Tsinghua Center for Astrophysics, Tsinghua University, Beijing 100084, China.
- <sup>17</sup>Saitama University, Saitama 338-8570, Japan.
- <sup>18</sup>Advanced Media Network Center, Utsunomiya University, Utsunomiya 321-8585, Japan.
- <sup>19</sup>National Institute of Informatics, Tokyo 101-8430, Japan.
- <sup>20</sup>Sakushin Gakuin University, Utsunomiya 321-3295, Japan.
- <sup>21</sup>Tokyo Metropolitan College of Industrial Technology, Tokyo 116-8523, Japan.
- <sup>22</sup>Max-Planck-Institut für Physik, München D-80805, Deutschland.

Received \_\_\_\_\_; accepted \_\_\_\_\_

---

<sup>23</sup>College of Industrial Technology, Nihon University, Narashino 275-8576, Japan.

<sup>24</sup>Shonan Institute of Technology, Fujisawa 251-8511, Japan.

<sup>25</sup>RIKEN, Wako 351-0198, Japan.

<sup>26</sup>Institute of Disaster Prevention Science and Technology, Yanjiao 065201, China.

<sup>27</sup>School of General Education, Shinshu University, Matsumoto 390-8621, Japan.

<sup>28</sup>Center of Space Science and Application Research, Chinese Academy of Sciences, Beijing 100080, China.

## ABSTRACT

We analyze the large-scale two-dimensional sidereal anisotropy of multi-TeV cosmic rays by Tibet Air Shower Array, with the data taken from 1999 November to 2008 December. To explore temporal variations of the anisotropy, the data set is divided into nine intervals, each in a time span of about one year. The sidereal anisotropy of magnitude about 0.1% appears fairly stable from year to year over the entire observation period of nine years. This indicates that the anisotropy of TeV Galactic cosmic rays remains insensitive to solar activities since the observation period covers more than a half of the 23rd solar cycle.

*Subject headings:* cosmic rays — diffusion — ISM: magnetic fields — solar neighborhood — Sun: activity

## 1. Introduction

Galactic cosmic rays (GCRs) are high-energy nuclei (most protons) which are believed to be accelerated by supernova remnants (SNRs) in our Galaxy and continuously reach the Earth after propagating in the Galaxy and heliosphere. The intensity of GCRs is nearly isotropic due to deflections in the Galactic magnetic field (GMF). However, extensive observations do show that there exists a slight anisotropy on the overall isotropic background (e.g. Jacklyn 1966; Nagashima et al. 1975; Cutler et al. 1981; Nagashima et al. 1989; Aglietta et al. 1996; Munakata et al. 1997; Amenomori et al. 2006; Abdo et al. 2009; Abbasi et al. 2009).

The large-scale sidereal cosmic ray (CR) anisotropy may arise from several causes. Firstly, it may result from the uneven distribution of CR sources such as SNRs and the process of CR propagation in the Galaxy. Using the diffusion model, it is expected that the amplitude of anisotropy satisfies  $A \sim D(R) \sim R^{1/3}$ , where  $D(R)$  is the diffusion coefficient which depends on the rigidity  $R$  of charged particles (e.g. Berezhinsky 1990; Shibata et al. 2004). Thus one can expect that the anisotropy amplitude will increase with energy. However, the observation of the anisotropy above hundreds of TeV is smaller than what is expected. It has been suggested that a nearby (within 1-2 kpc from the Sun) source in the opposite direction against the global CR diffusion may suppress the expected large amplitude to some degree (Erlykin et al. 2006). Other factors such as the complicated composition of CRs and isotropic CRs from the Galactic halo can also be helpful for reducing the anisotropy (e.g. Erlykin et al. 2006; Ptuskin et al. 2006). Secondly, the anisotropy can also be induced through both large-scale and local magnetic field configurations, possibly including effects of the heliosphere. Therefore, it is a useful tool to probe the local interstellar space surrounding the heliosphere and the magnetic structure of the heliosphere (Amenomori et al. 2007; Munakata et al. 2008; Amenomori et al. 2009). In

addition, an expected anisotropy is caused by the relative motion between the observer and the CR plasma, known as the Compton-Getting (CG) effect (Compton & Getting 1935). By analyzing the events recorded by the Tibet III Air Shower experiment, Amenomori et al. (2006) showed that GCRs corotate with the local GMF environment according to the null result of the Galactic CG effect. The CG modulation due to the Earth’s orbital motion around the Sun has been successfully detected by several GCR experiments in multi-TeV energy ranges (e.g. Cutler & Groom 1986; Amenomori et al. 2004, 2006; Abdo et al. 2009).

From the analysis of numerous experiments, it can be seen that both the amplitude and the phase of the best-fit first harmonic vary with CR energy in a wide range from tens of GeV to PeV (Guillian et al. 2007; Abbasi et al. 2009). Below several tens of GeV, solar modulation effects are most notable for GCRs. GCRs interact with the solar wind magnetic field, both an ordered field and irregular field components, after entering the heliosphere. The spatial distribution of GCRs can reflect the magnetic structure in the solar wind. With increasing energy, CRs become less sensitive to the solar modulation. It is well known that the flux of GCRs with energy per nucleon in the energy range of  $\sim 10^{11} - 10^{14}$  eV has a sidereal anisotropy of the order  $O(10^{-3})$ . The gyro radius  $r_L$  of CRs in this energy range in a GMF of  $3 \mu\text{G}$  is about several AU–0.03 pc, which is much smaller than the size of the Galaxy. In the multi-TeV range, the gyro radius of hundreds of AU becomes comparable to the spatial scale of the heliosphere in the nose direction toward the upstream side of the interstellar medium flow (e.g. Washimi & Tanaka 1996). However, it is known that the heliosphere has a long heliotail, the modulation in the heliotail remains possible. Therefore, the large-scale sidereal anisotropy of CRs in this energy range gives us an important clue about the magnetic field structure of the heliosphere or the local interstellar space surrounding the heliosphere.

The solar cycle shows a quasi-period of about 11 yr and the global magnetic polarity

reverses with a quasi-period of two solar activity cycles (e.g. Solanki et al. 2006). Since GCRs are modulated by solar activities in the given energy range mentioned above, it might be expected that the sidereal anisotropy may follow the variation of solar cycle. There have been many experiments devoted to the study of temporal variations of GCR sidereal anisotropy. Nagashima et al. (1989) found that both the amplitude and the phase of the sidereal anisotropy with the rigidity  $\sim 10^{13}\text{V}$  had no significant changes for more than ten years, except that the phase changed at the epoch (1979-1980) when the polar magnetic field of the Sun reversed its polarity. At primary energy as low as 2 TeV, Kozyarivsky et al. (1995) demonstrated that the sidereal anisotropy was constant within the accuracy of the experiment, with observations in the subsequent ten years (1982-1991) after this epoch of polarity reversal. Recently, underground muon observations showed that yearly mean harmonic vectors of the sidereal anisotropy in the sub-TeV region are more or less stable in phase and amplitude over 20 years since 1985 without showing any significant correlation with the solar activity and magnetic-cycles (Munakata et al. 2008). However, Milagro experiment recently reported an amplitude increase of the sidereal anisotropy at 6 TeV in the latter half of the 23rd solar cycle (from 2000 July to 2007 July), while the phase remains stable (Abdo et al. 2009). The contradiction needs further checks from other experiments.

Covering almost the same field of view and with similar sensitive energy range, the Tibet AS $\gamma$  experiment seemingly observed no variation in the sidereal anisotropy using data from both Tibet HD and Tibet III array which was divided into two parts by the solar maximum around 2001 (Amenomori et al. 2006). In the multi-TeV region, Amenomori et al. (2005a) found that both the amplitude and phase of the first harmonic vector of the daily variation are remarkably independent of primary energy. Taking advantage of the large field of view and high count rates as well as the good angular resolution of the incident direction, the Tibet III Air Shower Array provides currently the world's highest precision two-dimensional measurement of GCR intensity in this energy range. The observation

period runs from 1999 November to 2008 December, covering more than a half of the 23rd solar activity cycle from the maximum to the minimum. Therefore, we can do more precise study on the sidereal anisotropy variation year by year in correlation with the solar activity cycle. In this paper, we analyze temporal variations of sidereal anisotropy of multi-TeV GCR intensity using the data of Tibet III array from 1999 November to 2008 December. At this point, we cannot investigate the influence of the polarity reversal of the global solar magnetic field on the sidereal anisotropy due to the lack of data before the current magnetic field reversal. Note that we do not use the data of Tibet HD to perform the year-by-year analysis due to the limitation of the statistics, although it covers the period before the reversal.

## 2. Tibet Air Shower Array Experiment

The Tibet Air Shower Array experiment has been operating successfully at Yangbajing (90.522° E, 30.102° N; 4300 m above the sea level) in Tibet, China since 1990. The array has been gradually upgraded by increasing the number of counters from the Tibet-I array with 65 plastic scintillation detectors placed on a lattice with a 15 m spacing (Amenomori et al. 1992). The Tibet III array was completed in the late fall of 1999 (Amenomori et al. 2002). The array is composed of 497 fast timing (FT) detectors and 36 density (D) detectors, covering a surface area of 22,050 m<sup>2</sup>. Each FT detector equipped with a plastic scintillator plate and a 2 inch photomultiplier tube has a cross sectional area of 0.5 m<sup>2</sup> and is deployed at a lattice with a 7.5 m spacing. A 0.5 cm thick lead plate is placed on top of each counter in order to increase the detector array sensitivity by converting  $\gamma$  rays into electron-positron pairs. A CR event trigger signal is issued when any fourfold coincidence occurs in the FT counters recording more than 0.6 particles, resulting in a trigger rate of about 680 Hz at a few-TeV threshold energy. The shower size  $\sum \rho_{\text{FT}}$  is regarded as an estimator for the



primary particle energy, where the size of  $\sum \rho_{\text{FT}}$  is defined as the sum of particles per  $\text{m}^2$  for each FT detector. During 2002 and 2003, the inside area of the Tibet-III array was further enlarged to  $36,900 \text{ m}^2$  by installing additional 256 detectors. This full Tibet III array has been operating successfully since 2003. In the present analysis, to keep the uniformity of the data quality throughout the entire observation period from 1999 to 2008, we reconstructed CR air shower events obtained using the configuration of detectors which was completed in the late fall 1999 even for the full Tibet-III array.

In the present analysis, CR events are selected based on the following four criteria: (1) estimated air shower core location should be inside the array; (2) the zenith angle of the incident direction should be less than  $45^\circ$ ; (3) any fourfold coincidence in the FT counters should record a signal of more than 0.8 particles; (4) when  $10 \leq \sum \rho_{\text{FT}} < 178$  is satisfied, corresponding to a modal energy of about 5 TeV.

In total, about  $4.91 \times 10^{10}$  CR events are used in the present analysis.

### 3. Analysis and Results

Sitting on an almost horizontal plane, the Tibet III Air Shower Array has almost azimuth-independent efficiency in receiving GCR shower events for any given zenith angle. Therefore, the equi-zenith angle method is adopted in the present analysis. In brief, for a candidate “on-source window”, GCR air shower events recorded simultaneously in the side band of the same zenith angle belt can be used to construct the “off-source windows” and to estimate the background events. This method can eliminate various detection effects caused by instrumental and environmental variations, such as changes in pressure and temperature which are hard to be controlled and tend to introduce systematic errors in measurement.

With the large statistics, we can construct a two-dimensional sky map to reveal detailed

structural information of the large-scale GCR variations beyond the simple one-dimensional profile along the time scale. The idea of this method is that for each short time step (e.g. 8 minutes in the present analysis), for all directions, if we scale down (or up) the number of observed events by dividing them according to their relative CR intensity, then statistically, those scaled observed numbers of events in a zenith angle belt should be equal anywhere. A total  $\chi^2$  can be built accordingly, and the relative intensity of CRs  $I$  and its error  $\Delta I$  in each direction can be solved by minimizing the  $\chi^2$  function (see Amenomori et al. (2005b) for more details). Given the fact that the detector can quickly scan the sky along right ascension direction as a result of the self rotation of the Earth, the intensities of CRs along right ascension direction are measured under the same condition for each declination belt. Therefore, the modulation along right ascension direction in each declination belt is accurate and irrelevant to the inhomogeneous efficiency of the detector. However, as having been pointed out by (e.g. Andreyev et al. 2008; Kozyarivsky et al. 2008), when comparing CR intensities among different declination belts, we need absolute efficiency calibration along declination direction which is unfortunately not possible for current experiments. Once we have the absolute CR intensity in declination direction  $I_{dec,1D}(\delta)$ , we will obtain the true two-dimensional anisotropy map,  $I_{true,2D}(\alpha, \delta) = I_{quasi,2D}(\alpha, \delta) \times I_{dec,1D}(\delta)$ , here  $\alpha$  and  $\delta$  are right ascension and declination in the celestial coordinate respectively. Strictly speaking, the present analysis gives a combination of one-dimensional modulation curves in a fine set of declination bins –  $I_{quasi,2D}(\alpha, \delta)$  (For simplicity, we will omit the subscript of  $I_{quasi,2D}$  in the following text).

Using Lomb-Scargle Fourier transformation method (Lomb 1976; Scargle 1982) with CR data recorded by the Tibet III array, Tibet AS $\gamma$  experiment showed that besides the well-known solar diurnal, sidereal diurnal and sidereal semi-diurnal modulations at a level of  $\sim 10^{-3}$ , no other periodicity was found to have high enough significance from 1 hour to 2 years in the energy range from  $\sim 3.0$  TeV to  $\sim 12.0$  TeV (Li et al. 2008). The sidereal daily

variation can be described by the first and second harmonics and the solar daily variation can be described by the first harmonic alone. When applying the above mentioned method to data, the fit function is natural to contain both sidereal time and solar time modulation components. The other alternative method we used to separate modulations was to properly fold the data according to the sidereal time or solar time periodicity. This method was used in (Amenomori et al. 2005b, 2006) when we analyzed CR intensity variations in the sidereal time frame with several years data samples. Using this method, each event had to be re-weighted to form an exactly one year long and uniformly distributed data series before folding. Therefore, the disadvantage of this method is that more than one year’s data are needed, which can not be followed in current work. In this case, we adopt a new method of fitting all modulation components simultaneously to perform the year-by-year analysis of CR anisotropy.

Based on the results of Lomb-Scargle Fourier transformation, in the present analysis, we assume that at any moment  $t$ , the relative intensity of CRs at any given direction  $(\theta, \phi)$  in the horizontal coordinate, is modulated as a product of  $I_{sid}(\alpha_{sid}, \delta_{sid})$  and  $I_{sol}(\alpha_{sol}, \delta_{sol})$ . Here  $(\alpha_{sid}, \delta_{sid})$  and  $(\alpha_{sol}, \delta_{sol})$  are positions corresponding to the celestial coordinate in the local sidereal time frame and the local solar time frame of the same point  $(t, \theta, \phi)$  in horizontal coordinate,  $I_{sid}$  and  $I_{sol}$  denote the CR intensity in the sidereal time frame and the solar time frame respectively. So substituting  $I$  by  $I_{sid}(\alpha_{sid}, \delta_{sid}) \times I_{sol}(\alpha_{sol}, \delta_{sol})$ , the total  $\chi^2$  can be written as

$$\chi^2 = \sum_{t, \theta, \phi} \left( \left\{ \frac{N_{obs}(t, \theta, \phi)}{I_{sid}(\alpha_{sid}, \delta_{sid}) \times I_{sol}(\alpha_{sol}, \delta_{sol})} - \frac{\sum_{\phi \neq \phi'} [N_{obs}(t, \theta, \phi') / (I_{sid}(\alpha'_{sid}, \delta'_{sid}) \times I_{sol}(\alpha'_{sol}, \delta'_{sol}))]}{\sum_{\phi \neq \phi'} 1} \right\}^2 \right. \\ \left. \times \left\{ \frac{N_{obs}(t, \theta, \phi)}{I_{sid}^2(\alpha_{sid}, \delta_{sid}) \times I_{sol}^2(\alpha_{sol}, \delta_{sol})} + \frac{\sum_{\phi \neq \phi'} [N_{obs}(t, \theta, \phi') / (I_{sid}^2(\alpha'_{sid}, \delta'_{sid}) \times I_{sol}^2(\alpha'_{sol}, \delta'_{sol}))]}{(\sum_{\phi \neq \phi'} 1)^2} \right\}^{-1} \right). \quad (1)$$

Here,  $N_{obs}(t, \theta, \phi)$  denotes the number of observed events in the “window”  $(\theta, \phi)$  in the horizontal coordinate at the moment  $t$ . After minimizing the  $\chi^2$  function,  $I_{sid}(\alpha_{sid}, \delta_{sid})$  and  $I_{sol}(\alpha_{sol}, \delta_{sol})$  can be obtained simultaneously.

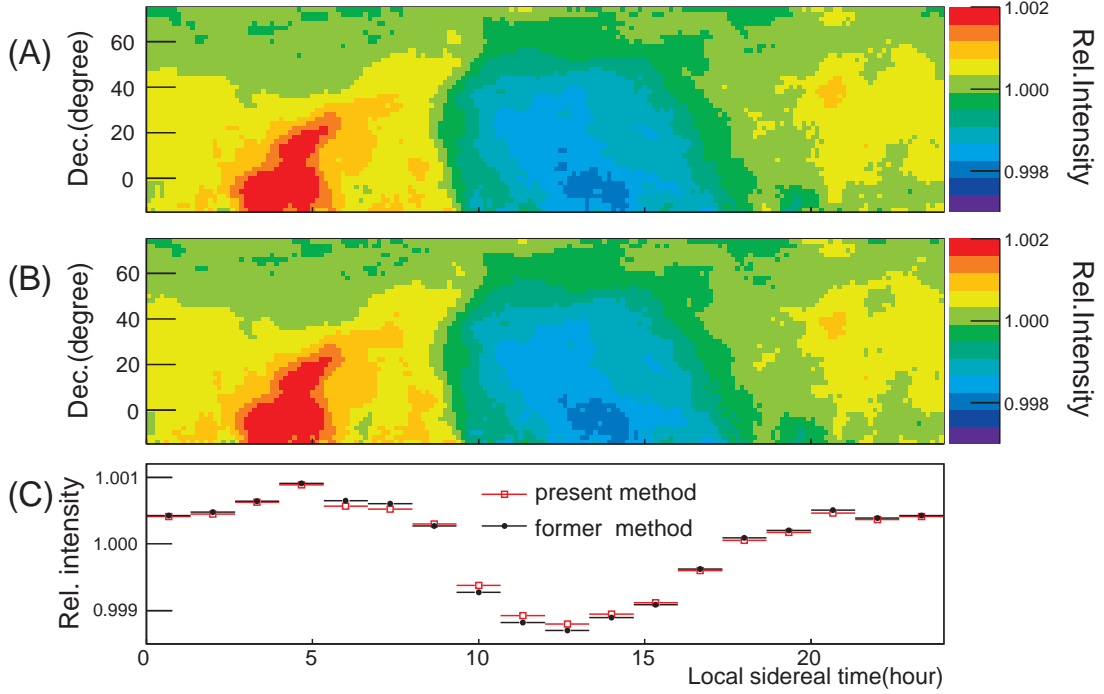


Fig. 1.— Sidereal diurnal variation of CR relative intensity with the representative primary energy of 5 TeV averaged over all nine phases of Tibet III Air Shower Array from Nov. 1999 to Dec. 2008. (A) 2D maps obtained with the present method mentioned as Equation (1); (B) 2D maps obtained with the former method used in (Amenomori et al. 2006); (C) the 1D projection of 2D maps averaged over all declinations for comparison.

The data were acquired by the Tibet III Air Shower Array for 1915.5 live days from Nov. 1999 to Dec. 2008. It covers all nine running phases of the Tibet III Air Shower Array. As described in Equation (1), for any direction in the horizontal coordinate at any moment in the observation period, a  $\chi^2$  function can be constructed. Covering all nine phases of Tibet III array, we got a total  $\chi^2$  accumulated over the entire observation period. By minimizing it, the CR intensity maps in the frame of the local sidereal time and the local solar time averaged over all nine phases were obtained simultaneously. Fig. 1 (A) shows the intensity map of GCRs with the modal energy of 5 TeV in the local sidereal

time frame averaged over the whole observation period of Tibet III array. The result is consistent with former observation results of Tibet III experiment by different methods (Amenomori et al. 2005a, 2006, 2007). The amplitude of the sidereal anisotropy is about 0.1%, and the maximum around 6 hr in the local sidereal time. The so-called “tail-in” and “loss-cone” anisotropy components (e.g. Nagashima & Mori 1976; Nagashima et al. 1998) are clearly shown in the map. The maximum phase shifts to earlier hours as the viewing declination moves southward in two-dimensional intensity map. The excess around the Cygnus arm direction can also be seen in the map.

For a detailed examination between the present method and the former method used in Amenomori et al. (2006), we constructed a two-dimensional map of CR relative intensity with former method used in Amenomori et al. (2006) with the same data samples, showed in Fig. 1 (B). The 1D projections of Fig. 1 (A) and (B) averaged over all declination belts ( $-14.89^\circ$  to  $75.11^\circ$ ) are displayed in Fig. 1 (C). From the comparison, it can be seen that the results agree with each other well.

To study the temporal variation of the sidereal anisotropy, the data was divided into nine subsets, corresponding to nine running phases of Tibet III array each in a time scale of about one year, as summarized in Table 1.

Using data samples recorded during each separated phase, the GCR relative intensity maps in the local sidereal time frame averaged over each phase were obtained according to Equation (1). The two-dimensional (2D) relative intensity maps of GCRs with modal energy around 5 TeV in the local sidereal time frame of different phases are displayed in Fig. 2, and the corresponding one-dimensional (1D) projections over all declinations are also shown. The solid red markers in each plot denote the relative intensities of GCRs in the local sidereal time frame over the corresponding observation period, while the blue dashed smooth curves in plots represent variations of GCR relative intensity averaged over

Table 1: Definition of nine phases of Tibet III from 1999 November to 2008 December

Phase	Start time	End time	Live days	Number of used CR events
1	Nov. 18, 1999	Jun. 29, 2000	173.1	$5.16 \times 10^9$
2	Oct. 28, 2000	Oct. 11, 2001	283.7	$8.14 \times 10^9$
3	Dec. 05, 2001	Sep. 19, 2002	201.8	$5.59 \times 10^9$
4	Nov. 18, 2002	Nov. 18, 2003	259.1	$6.34 \times 10^9$
5	Dec. 14, 2003	Oct. 10, 2004	123.6	$3.07 \times 10^9$
6	Oct. 19, 2004	Nov. 15, 2005	277.6	$6.79 \times 10^9$
7	Dec. 07, 2005	Nov. 03, 2006	114.5	$2.71 \times 10^9$
8	Nov. 06, 2006	Feb. 25, 2008	269.2	$6.36 \times 10^9$
9	Mar. 02, 2008	Dec. 03, 2008	212.9	$4.91 \times 10^9$

all nine phases of Tibet III array, the same as the bottom plot with the marker of “present method” in Fig. 1. From the comparison of GCR sidereal anisotropy in different phases from 1999 November to 2008 December, it can be seen that the CR intensity variation in the local sidereal time appears fairly stable year by year.

Furthermore, we take a  $\chi^2$  test to check the consistency among different phases. As shown in Equation (1), the CR intensity variation along the local sidereal time averaged over all nine phases contains contributions of each single phase. To avoid the correlation between the two plots which are used in the test, we compare the result of each single phase with the average one of all the other eight phases except the single one instead of the average one of all nine phases. The obtained  $\chi^2/ndf$  value and the probability of each comparison were labeled in Fig. 2. The test also indicates stability for the sidereal anisotropy with time.

The observation period of Tibet III Array covers more than a half of the 23rd solar activity cycle from the maximum to the minimum. So it implies that the sidereal anisotropy

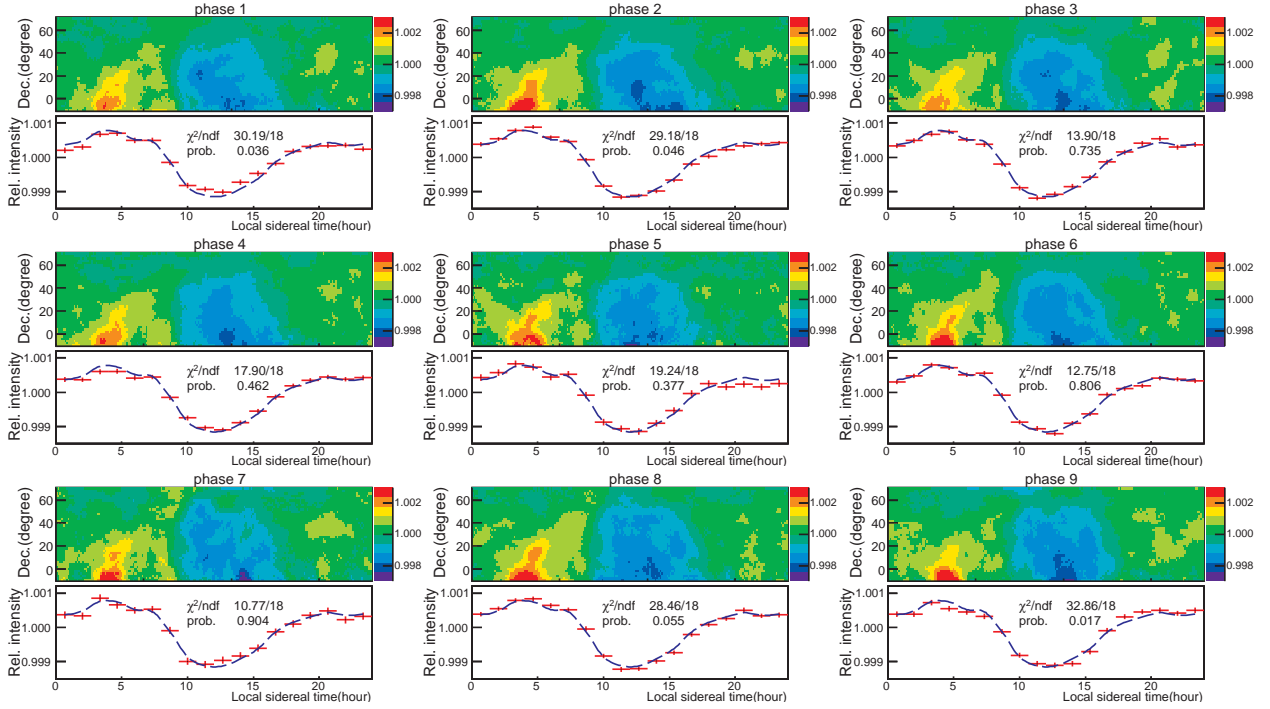


Fig. 2.— Cosmic ray intensity variation in the local sidereal time frame for CRs with the modal energy around 5 TeV in the 9 phases of Tibet III Array. Top: 2D intensity map of each phase; Bottom: 1D projection averaged over all declinations. In bottom plots of each panel, the red crosses in each plot show the intensity variation over each phase respectively, while the dashed blue lines represent the intensity averaged over all nine phases of Tibet III array.

of multi-TeV GCRs is insensitive to the solar activity. It disagrees with the recent result of Milagro experiment (Abdo et al. 2009), which shows an increase in the amplitude of the sidereal anisotropy with time while the phase remains stable.

#### 4. Conclusions

In this work, we investigate temporal variations of the large-scale sidereal anisotropy of GCR intensity using the data of Tibet III Air Shower Array from 1999 November to 2008 December. Totally  $\sim 4.91 \times 10^{10}$  CR events are used. The data is divided into nine intervals, each in a time span of about one year. We find that, in the multi-TeV energy range, the sidereal anisotropy is fairly stable year by year over all nine phases of Tibet III Array, which covers more than a half of the 23rd solar cycle from the maximum to the minimum. It indicates that the anisotropy in this energy range appears insensitive to solar activities. This feature can give some constraints on the origin of the sidereal anisotropy, which has no convincing and widely accepted explanations so far.

#### 5. Acknowledgements

The collaborative experiment of the Tibet Air Shower Arrays has been performed under the auspices of the Ministry of Science and Technology of China and the Ministry of Foreign Affairs of Japan. This work was supported in part by Grants-in-Aid for Scientific Research on Priority Areas (712) (MEXT), by the Japan Society for the Promotion of Science (JSPS), by the National Natural Science Foundation of China, the Chinese Academy of Sciences and the Ministry of Education of China. C. Fan is partially supported by the Natural Science Foundation of Shandong Province, China (No.Q2006A02).



## REFERENCES

- Abbasi, R. U., et al. 2009, arXiv:0907.0498
- Abdo, A. A., et al. 2009, *ApJ*, 698, 2121
- Aglietta, M., et al. 1996, *ApJ*, 470, 501
- Amenomori, M., et al. 1992, *Phys. Rev. Lett.*, 69, 2468
- Amenomori, M., et al. 2002, *Proc. 27th Int. Cosmic Ray Conf. (Hamburg)*, 2, 573
- Amenomori, M., et al. 2004, *Phys. Rev. Lett.*, 93, 061101
- Amenomori, M., et al. 2005, *ApJ*, 626, L29
- Amenomori, M., et al. 2005, *ApJ*, 633, 1005
- Amenomori, M., et al. 2006, *Science*, 314, 439
- Amenomori, M., et al. 2007, *AIP Conf. Proc.*, 932, 283
- Amenomori, M., et al. 2009, *Proc. 31st Int. Cosmic Ray Conf. (Lodz)*, icrc0296
- Andreyev, Yu. M., Kozyarivsky, V. A. & Lidvansky, A. S. 2008, arXiv:0804.4381
- Berezinsky, V. S. 1990, *Proc. 21st Int. Cosmic Ray Conf. (Adelaide)*, 11, 115
- Compton, A. H. & Getting, I. A. 1935, *Phy. Rev.*, 47, 817
- Cutler, D. J., Bergeson, H. E., Davies, J. F., & Groom, D. E. 1981, *ApJ*, 248, 1166
- Cutler, D. J. & Groom, D. E. 1986, *Nature Lett.*, 322, L434
- Erlykin, A. D., Wolfendale, A. W. 2006, *Astropart. Phys.*, 25, 183
- Guillian, G., et al. 2007, *Phys. Rev. D*, 75, 062003

- Jacklyn, R. M. 1966, *Nature*, 211, 690
- Kozyarivsky, V. A., et al. 1995, *Bull. Russ. Acad. Sci., Phys.*, 59, 714
- Kozyarivsky, V. A. & Lidvansky, A. S. 2008, *Astron. Lett.*, 34, 113
- Li, A. F., et al. 2008, *Proc. 30th Int. Cosmic Ray Conf. (Mexico City)*, 1, 609
- Lomb, N. R. 1976, *Astrophys. Space Sci.*, 39, 447
- Munakata, K., et al. 2008, arXiv:0811.0422v2
- Munakata, K., et al. 1997, *Phys. Rev. D*, 56, 23
- Nagashima, K., et al. 1975, *Proc. 14th Int. Cosmic Ray Conf. (Munich)*, 4, 1503
- Nagashima, K., Mori, S. 1976, *Proc. Int. Cosmic Ray Symp. on High Energy Cosmic Ray Modulation (Tokyo)*, 326
- Nagashima, K., et al. 1989, *Nuovo Cimento C*, 12, 695
- Nagashima, K., Fujimoto, K., Jacklyn, R. M. 1998, *J. Geophys. Res.* 103, 17429
- Ptuskin, V. S. , Jones, F. C., Seo, E. S. & Sina, R. 2006, *Adv. Space Res.*, 37, 1909
- Scargle, J. D. 1982, *ApJ*, 263, 835
- Shibata, T., Hareyama, M., Nakazawa, M. & Saito, C. 2004, *ApJ*, 612, 238
- Solanki, S. K., Inhester, B., & Schüssler, M. 2006, *Rep. Prog. Phys.*, 69, 563
- Washimi, H., & Tanaka, T. 1996, *Space Sci. Rev.*, 78, 85